3D INTRAVASCULAR ENDOSCOPY USING CT

Haris Huseinagić
Radiology and Interventional Radiology Department, Medical Institute Bayer, Tuzla, Bosnia and Hercegovina

Irma Rušidović
Pharma Maac d.o.o., Sarajevo, Bosnia and Hercegovina

Amir Arnaut
Radiology and Interventional Radiology Department, Medical Institute Bayer, Tuzla, Bosnia and Hercegovina

Sadik Mujabašić
Radiology and Interventional Radiology Department, Medical Institute Bayer, Tuzla, Bosnia and Hercegovina

ABSTRACT

Coronary CT angiography can be used to characterize coronary plaques based on both morphology and composition.

Coronary plaques are typically evaluated with 2D axial and multiplanar reformatted images. However, these visualization tools are limited to observing extraluminal changes in coronary arteries. The presence of plaque precludes visual visualization of the coronary artery wall within the lumen.

Since its invention in 2000, coronary fly-through or virtual angioscopy (VA) has been widely studied. However, its application has been limited by the need for optimal computed tomography (CT) acquisition and time-consuming post-processing.

In recent years, advances in post-processing software have simplified its VA design, but until recently, image quality was insufficient for most patients.

3D angioscopy visualization (3DIE) is used to visualize the different coronary artery linings and plaque appearances associated with different plaque types.

Keywords: Coronary CT angiography, coronary artery disease, plaque, 3D intravascular endoscopy, visualization

INTRODUCTION

Coronary CT angiography (CCTA) is a well-established minimally invasive imaging modality for the diagnosis of coronary artery disease (CAD), and many studies have reported high diagnostic value [(1-5)]. CCTA can characterize coronary artery plaque with respect to its plaque components and can also detect and evaluate coronary artery stenosis [(6-8)]. It is generally believed that plaque composition, rather than the degree of luminal stenosis, may provide

more accurate information for predicting a patient's risk of future cardiac events [(1)] .

Since its first mention in 2000, coronary fly-through or 3D endovascular endoscopy (3DIE) using different generations of computed tomography (CT) devices has been reported in many publications [(9,10)]. The main reasons for limited research on this topic have been the requirements for optimal CT scanning and time-consuming post-processing. Recent advances in post-processing software have facilitated the design of 3D endovascular endoscopy (3DIE). The introduction of multidetector CT (MDCT)

improved temporal resolution, which showed more stable data quality in all patients.

Coronary plaques are typically evaluated using 2D axial and multiplanar reformatted images in addition to 3D volume-rendered images. The main limitation of these visualizations is that the appearance of the plaque and associated changes in the coronary artery wall cannot be observed directly within the lumen. This limitation is overcome by 3D angioscopy (3DIE), a proven 3D visualization technique for diagnostic applications in cardiovascular diseases [(11-15)].

MATERIALS AND METHODS

A total of 121 patients (95 males, mean age 60 ± 13 years) whose coronary arteries were scanned with MDCT using a standard coronary artery protocol (uWS Work-CT station from Shanghai United Imaging Healthcare Co., Ltd.) Randomly selected., GMBH.).

Allergy to iodinated contrast media, renal insufficiency (creatinine level > 120 mol/L), pregnancy, hemodynamic instability, and previous stent graft or bypass surgery were all exclusion criteria for DSCT.

Patients with elevated or irregular heart rates were not excluded in this study. Our local ethics committee approved the study protocol, and all participating patients provided written informed consent.

No beta-blockers were administered prior to the study, regardless of individual heart rate or heart rate variability.

All patients underwent CCTA with retrospective ECG gating on a 160 multislice CT (MSCT) (uCT 780, Shanghai United Imaging Healthcare Co., LTD).

NON-INVASIVE CORONARY ANGIOGRAPHY AND VIRTUAL CORONARY ANGIOSCOPY

For MSCT, we used a uCT 780 scanner (Shanghai United Imaging Healthcare Co., LTD) with a 1024 × 1024 high-resolution reconstruction matrix and ECG-guided cardiac phase-selective image reconstruction. 90 ml of contrast agent (370 mg/ml) was injected into the elbow vein at 4 ml/s through an 18-gauge catheter, followed by a contrast-enhanced scan (collimation 1.0

mm, step size 1.5, 120 kV, 300 mA, rotation time 500 ms). (16)

All scans were performed during his single 5-second breath-hold. The raw scan data was then reconstructed using an ECG-guided multislice spiral reconstruction algorithm (16). The optimized image reconstruction time point was

determined in a series of tests. In our series, image reconstruction was performed during diastole using retrospective ECG gating with a 38–50% delay after R-wave onset for the right coronary artery and a 50% delay for the left coronary artery.

150–200 axial image slices were reconstructed using slice increments of 0.625 mm and matrix size of 1024 × 1024, covering the entire cardiac volume with nearly isotropic spatial resolution (0.25 × 0.25 × 0.5 mm). The field of view of the image reconstruction is adjusted to the heart volume (ranging from 150 to 200 mm), and the pixel size ranges from 0.29 to 0.29 mm to 0.39 to 0.39 mm. The image data were reconstructed and transferred to a computer workstation (uWS Work-CT station (Shanghai United Imaging Healthcare Co., LTD.)) for post-processing. When 3D volume rendering is performed, the image data is divided into 3D voxels, each with a different density value, expressed in Hounsfield units (HU).

Simultaneous display of CCTA reports, CT IVUS, multiplanar reformatting (MPR three-dimensional volume rendering model), 3D flow analysis, and endoscopic views enable precise interactive perspective navigation (Figure 1). The navigator is initially placed in the area of interest. Automatic path definition finds the most direct route from one target point to another, giving the impression of flying through the lumen of a coronary artery.

The scan protocols for these CT scanners are as follows: Detector collimation 2 x 32 x 0.6 mm, gantry rotation 0.33 seconds, tube voltage 100-120 kVp (BMI) and 345-420 mAs/rev depending on tube current range. Detector collimation

160 x 0.5 mm, gantry rotation 0.25 seconds, tube voltage 100-120 kVp (depending on BMI and automatic tube). Current modulation of 160-slice CT. For a 160-slice CT, a beta-blocker was administered to the patient whose heart rate exceeded 90 beats per minute.

Iopromide (370 mg/ml, Bayer Schering Pharma) was administered using a dual-head motorized injector with bolus tracking technology and increasing the CT attenuation of 130 Hounsfield units (HU) as the trigger threshold for scan initiation, injected into the aorta. In the 120 kV protocol, 90 mL of contrast medium was injected at a rate of 4.5–5.5 mL/s. All injections were followed by a 30 ml saline rinse. ECG tube current modulation was used with total tube current between 30% and 75% of the R-R interval. For the DSCT protocol, the pitch ranged from 0.2 to 0.4 and was determined by heart rate. For DSCT, images were reconstructed with slice thicknesses of 0.6–0.75 mm and steps of 0.5–0.6 mm.

Post-processing was performed on a uWS Work CT station (Shanghai United Imaging Healthcare Co., LTD.). This software allows semi-automated fly-through of small vessels, providing anterior and posterior internal views as well as views of their course and location on the surface of the heart (Figure 2). - Additionally, three multiplanar reconstruction planes (sagittal, coronal, and axial) are displayed for the camera position. The distance travelled for each main branch was recorded in millimetres, and the time taken to complete the assessment for each main branch was also recorded in minutes. Although the ostium of the side branch was visualized, a fly-through of the side branch was not performed.
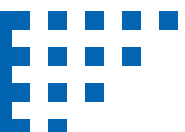
CCTA FINDINGS IN CORONARY ARTERY DISEASE AND CORONARY STENTING

Coronary plaques were most commonly found in the left anterior descending (LAD) coronary artery in 42 patients (35%), the LAD and left circumflex (LCX) in 30 patients (25%), all three main coronary vessels in 24 patients (20%), and the right coronary artery (RCA) in 12 patients (10%). In the remaining 13 patients (10%), plaques involving both the LAD and the RCA were discovered.

CCTA findings with patent coronary stents were found normal in 10 of 16 patients treated with coronary stents, while in-stent restenosis was suspected in the remaining 6 patients. A total of 11 stents were placed in the coronary arteries of 10 patients with patent stents, with 7 in the LAD, 3 in the RCA, and 1 in the LCX. A total of six stents were placed in the coronary arteries of five patients with suspected in-stent restenosis, three in the LAD, two in the LCX, and one in the RCA.

Table 1 lists patient features and cardiovascular risk factors.

3D INTRAVASCULAR ENDOSCOPY (3DIE) IMAGE GENERATION

CT volume data were generated from the original DICOM images and transferred to a workstation equipped with uWS-CT version R004 (Shanghai United Imaging Healthcare Co., LTD) for 3D imaging of endovascular endoscopy (3DIE).

The CT data were post-processed using the CT value thresholding technique [(17)]. In summary, the first step is to measure the CT attenuation of the major coronary arteries, specifically the right and left coronary arteries, to determine the threshold used to remove contrast-enhanced blood from the coronary arteries. CT thresholds determined between 200 and 350 HU in the first step were used to create endoluminal views of the coronary ostium, luminal surface, and coronary plaque. After determining the average threshold, increase the upper threshold by 20 HU to detect changes in the coronary wall and plaque surface.

This prevents floating shapes and other artifacts from appearing in the final (3DIE) image. If an inappropriate threshold is selected, the presence of artifacts can cause irregular or distorted intraluminal appearance of the coronary ostium or plaque, which can affect the visualization and evaluation of coronary lesions.

Because the diameter of coronary arteries is relatively small (3–5 mm), to see the exact anatomical details, the intraluminal appearance of the coronary ostium and plaque shown in the 3DIE images should be compared and associated with the corresponding an orthogonal view (Figure 3). This accurately identifies both normal anatomy and abnormal wall changes.

NORMAL CORONARY ARTERY WALL (3DIE) APPEARANCES

In 3DIE, the coronary artery wall appears smooth, without the presence of coronary plaque or atherosclerotic changes, and the coronary ostial configuration and lumen of a normal coronary artery are clearly demonstrated. Figure 4 shows the normal endoluminal appearance of the left coronary artery ostium, corresponding to the various branches arising from the left coronary artery and the normal right coronary ostium, as seen in 3DIE visualization.

CORONARY PLAQUE (3DIE) APPEARANCES

The appearance of a plaque and the resulting changes in the coronary artery wall are determined by the type, composition, and extent of the plaque. Additionally, the location or position of the plaque relative to the artery wall can be assessed for eccentric or concentric appearance, as well as whether the coronary ostium is covered by the plaque.

The following sections show 3DIE appearances associated with various types of plaques.

PLAQUES THAT HAVE NOT BEEN CALCIFIED

Non-calcified plaques are commonly seen on (3DIE) as smooth protruding signs emanating from the coronary artery wall (Figure 5). Because the CT attenuation of non-calcified plaques is much lower than that of contrast-enhanced blood in coronary arteries, changing the CT threshold when moving the viewing position from a normal coronary artery to a location where a coronary artery is present is useful and important for detection. - Plaque associated with surrounding coronary ostia, non-calcified plaque.

PLAQUES THAT HAVE BEEN CALCIFIED

In 3DIE, calcified plaques usually appear as prominent signs with a smooth appearance. The position or location of the plaque relative to the arterial wall can be accurately assessed by changes in eccentric (Figure 6) or concentric appearance or lumen with respect to involvement of the upper or lower part of the wall. In 3DIE, most calcified plaques appear as smooth protruding appearances, as shown in Figure 7. On the other hand, the presence of highly calcified plaques along the coronary arteries can lead to irregular intraluminal changes in the coronary artery walls.

Figure 8 shows visualization of a patient with extensive calcification in the RCA, LM, LAD, and LCX and an irregular intraluminal appearance in the coronary artery wall.
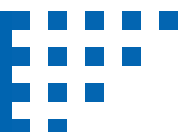
MIXED PLAQUES

Plaque contains a variety of components, which often results in an irregular appearance within the lumen. This suggests that coronary artery walls undergo multiple stages of remodelling, including a stable phase during which calcified plaques form and an unstable phase during which non-calcified plaques containing lipid-rich components are deposited. Figure 9 shows a mixed plaque in the proximal segment of the LAD, with non-calcified components making up the majority of the content. The corresponding 3DIE shows irregular intraluminal changes in the coronary artery wall caused by mixed plaque.

3DIE VISUALIZATION OF CORONARY STENTS

3DIE visualization has been reported to be a potential tool for endovascular stent implantation and stent follow-up as it can visualize the intraluminal view of the arterial wall and stent surface (15-20) .

STANDARD STENT APPEARANCES

Because the CT attenuation of coronary stents is much higher than that of contrast-enhanced blood, stent-on (3DIE) can be easily deployed as a dense structure with a uniform appearance within the coronary artery, depending on where the stent is deployed. It can be visualized in 3DIE visualization. Figure 10 shows an open coronary stent placed in the left anterior descending artery (LAD), with a smooth circular appearance.

SUMMARY AND CONCLUSION

We have shown a spectrum of 3DIE findings of coronary plaques and coronary stents in this pictorial essay, which includes both normal lumen appearances and pathological changes caused by plaques or stents. Although 3DIE is not recommended as a routine tool for the detection of coronary plaques or stents, it can be used in conjunction with conventional visualizations to provide an accurate assessment of coronary plaques and stents.

3DIE visualization has potential applications for assessing coronary plaques in terms of plaque characterization and intraluminal appearances, while in coronary stenting, 3DIE can demonstrate intraluminal coronary stents in relation to coronary ostia or detect luminal changes due to in-stent restenosis.

3DIE visualization is believed to be useful for better understanding the effect of coronary plaques and stents on the coronary wall and subsequent clinical outcomes [(12) (13)(15)].

This review`s 3DIE visualization tool could help overcome some of the image processing limitations for quantitative assessment of atherosclerotic plaques [(20)]. This table summarizes the main benefits of 3DIE visualization. However, further studies are needed to confirm the 3DIE results and their associated clinical value.

REFERENCES

1. Schuijf JD, Beck T, Burgstahler C, Jukema JW, Dirksen MS, De Roos A, et al. Differences in plaque composition and distribution in stable coronary artery disease versus acute coronary syndromes; non-invasive evaluation with multi-slice computed tomography. Acute Card Care. 2007;9(1):48– 53. https://pubmed.ncbi.nlm.nih.gov/17453539/

2. Vanhoenacker PK, Heijenbrok-Kal MH, Van Heste R, Decramer I, Van Hoe LR, Wijns W, et al. Diagnostic performance of multidetector CT angiography for assessment of coronary artery disease: meta-analysis. Radiology. 2007 Aug;244(2):419–28. https://pubmed.ncbi.nlm.nih.gov/17641365/

3. Sun Z, Lin CH, Davidson R, Dong C, Liao Y. Diagnostic value of 64-slice CT angiography in coronary artery disease: a systematic review. Eur J Radiol. 2008 Jul;67(1):78–84. https://pubmed.ncbi.nlm.nih.gov/17766073/

4. Abdulla J, Abildstrom SZ, Gotzsche O, Christensen E, Kober L, Torp-Pedersen C. 64-multislice detector computed tomography coronary angiography as potential alternative to conventional coronary angiography: a systematic review and meta-analysis. Eur Heart J. 2007 Dec;28(24):3042– 50. https://pubmed.ncbi.nlm.nih.gov/17981829/

5. Sun ZH, Cao Y, Li HF. Multislice computed tomography angiography in the diagnosis of coronary artery disease. J Geriatr Cardiol. 2011;8(2):104 –13. https://pubmed.ncbi.nlm.nih.gov/22783294/

6. Rodriguez-Granillo GA, Rosales MA, Degrossi E, Durbano I, Rodriguez AE. Multislice CT coronary angiography for the detection of burden, morphology and distribution of atherosclerotic plaques in the left main bifurcation. Int J Cardiovasc Imaging. 2007 Jun;23(3):389–92. https://pubmed.ncbi.nlm.nih.gov/17028928/

7. Schmid M, Pflederer T, Jang IK, Ropers D, Sei K, Daniel WG, et al. Relationship between degree of remodeling and CT attenuation of plaque in coronary atherosclerotic lesions: an in- vivo analysis by multi-detector computed tomography. Atherosclerosis. 2008 Mar;197(1):457–64. https://pubmed.ncbi.nlm.nih.gov/17727859/

8. Motoyama S, Kondo T, Sarai M, Sugiura A, Harigaya H, Sato T, et al. Multislice computed tomographic characteristics of coronary lesions in acute coronary syndromes. J Am Coll Cardiol. 2007 Jul 24;50(4):319–26. https://pubmed.ncbi.nlm.nih.gov/17659199/

9. Van Ooijen PMA, Nieman K, De Feyter PJ, Oudkerk M. Noninvasive coronary angioscopy using electron beam computed tomography and multidetector computed tomography. Am J Cardiol. 2002 Nov 1;90(9):998–1002. https://pubmed.ncbi.nlm.nih.gov/12398971/

10. Schroeder S, Kopp AF, Ohnesorge B, Loke-Gie H, Kuettner A, Baumbach A, et al. Virtual coronary angioscopy using multislice computed tomography. Heart. 2002;87(3):205 –9. https://pubmed.ncbi.nlm.nih.gov/11847152/
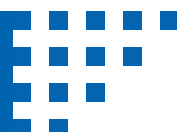
11. Sun Z, Zheng H. Effect of suprarenal stent struts on the renal artery with ostial calcification observed on CT virtual intravascular endoscopy. Eur J Vasc Endovasc Surg. 2004 Nov;28(5):534–42. https://pubmed.ncbi.nlm.nih.gov/15465376/

12. Sun Z, Dimpudus FJ, Nugroho J, Adipranoto JD. CT virtual intravascular endoscopy assessment of coronary artery plaques: a preliminary study. Eur J Radiol. 2010 Jul;75(1). https://pubmed.ncbi.nlm.nih.gov/19781885/

13. Sun Z. 3D multislice CT angiography in post-aortic stent grafting: a pictorial essay. Korean J Radiol. 2006;7(3):205–11. https://pubmed.ncbi.nlm.nih.gov/16969051/

14. Sun Z, Allen YB, Nadkarni S, Knight R, Hartley DE, Lawrence-Brown MMD. CT virtual intravascular endoscopy in the visualization of fenestrated stent-grafts. J Endovasc Ther. 2008 Feb;15(1):42–51. https://pubmed.ncbi.nlm.nih.gov/18254667/

15. Sun Z, Cao Y. Multislice CT angiography assessment of left coronary artery: correlation between bifurcation angle and dimensions and development of coronary artery disease. Eur J Radiol. 2011 Aug;79(2). https://pubmed.ncbi.nlm.nih.gov/21543178/

16. Kopp AF, Ohnesorge B, Flohr T, Georg C, Schröder S, Küttner A, et al. [Cardiac multidetector-row CT: first clinical results of retrospectively ECG-gated spiral with optimized temporal and spatial resolution]. Rofo. 2000 May 1;172(5):429–35. https://pubmed.ncbi.nlm.nih.gov/10874969/

17. Jodas DS, Pereira AS, Tavares JMRS. A review of computational methods applied for identification and quantification of atherosclerotic plaques in images. Expert Syst Appl. 2016 Mar 15;46:1 –14. https://doi.org/10.1016/j.eswa.2015.10.016

18. Sun Z, Al Dosari SA, Ng C, Al-Muntashari A, Almaliky S. Multislice CT virtual intravascular endoscopy for assessing pulmonary embolisms: a pictorial review. Korean J Radiol. 2010 Mar;11(2):222–30. https://pubmed.ncbi.nlm.nih.gov/20191070/

19. Sun Z. Coronary CT angiography in coronary artery disease: correlation between virtual intravascular endoscopic appearances and left bifurcation angulation and coronary plaques. Biomed Res Int. 2013;2013. https://pubmed.ncbi.nlm.nih.gov/24455719/

20. Ohnesorge B, Flohr T, Becker C, Kopp AF, Schoepf UJ, Baum U, et al. Cardiac imaging by means of electrocardiographically gated multisection spiral CT: initial experience. Radiology. 2000;217(2):564–71. https://pubmed.ncbi.nlm.nih.gov/11058661/
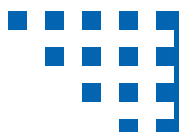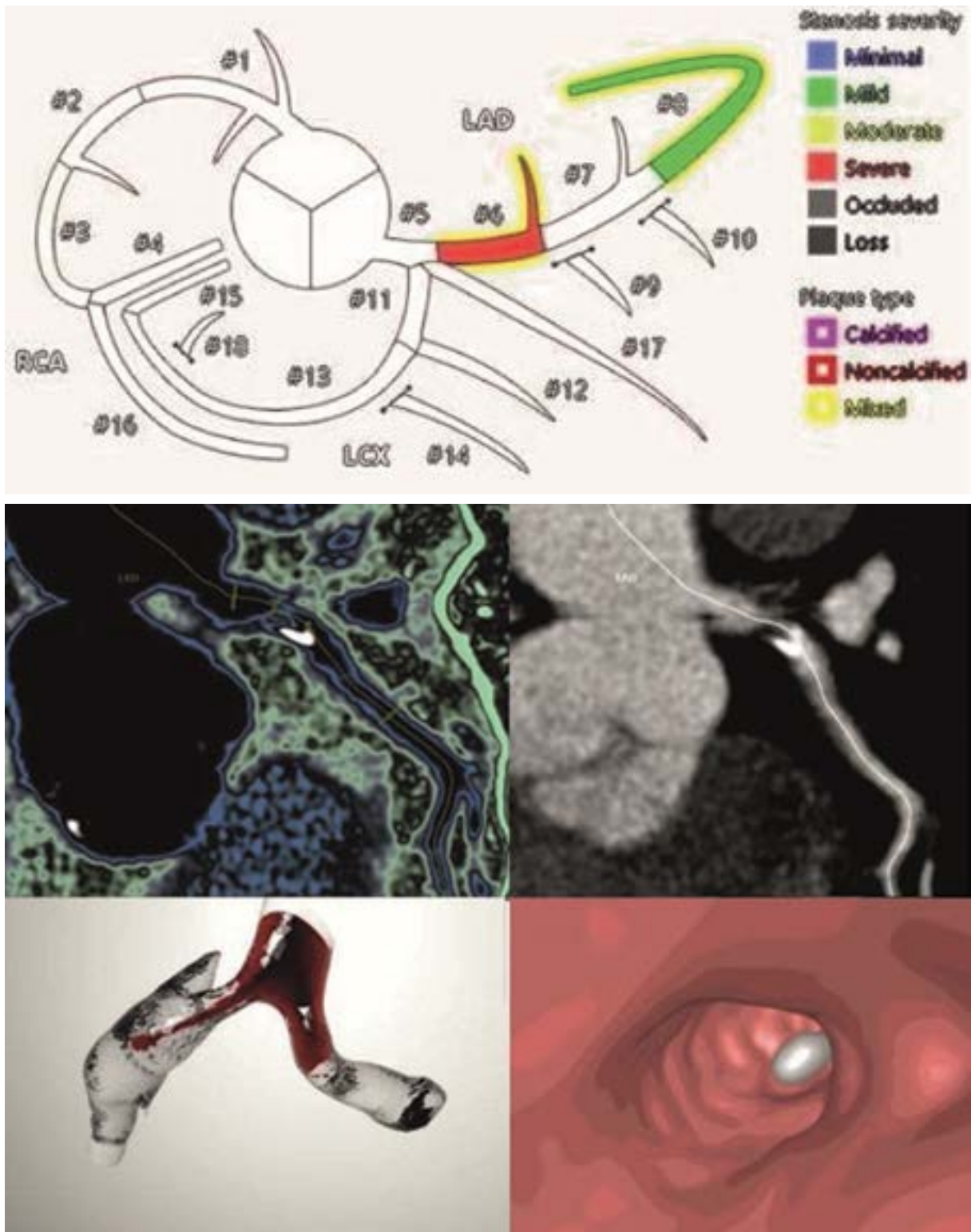
Figure 1. Correlation of VIE visualization and orthogonal views of coronary anatomy and plaque. Report sample (a), CTIVUS (b) and curved planar reformatted image (c) of the segment #6 LAD with mixed plaque, thrombus and calcium. 3D model with flow analysis of non-calcified stenosis (d).
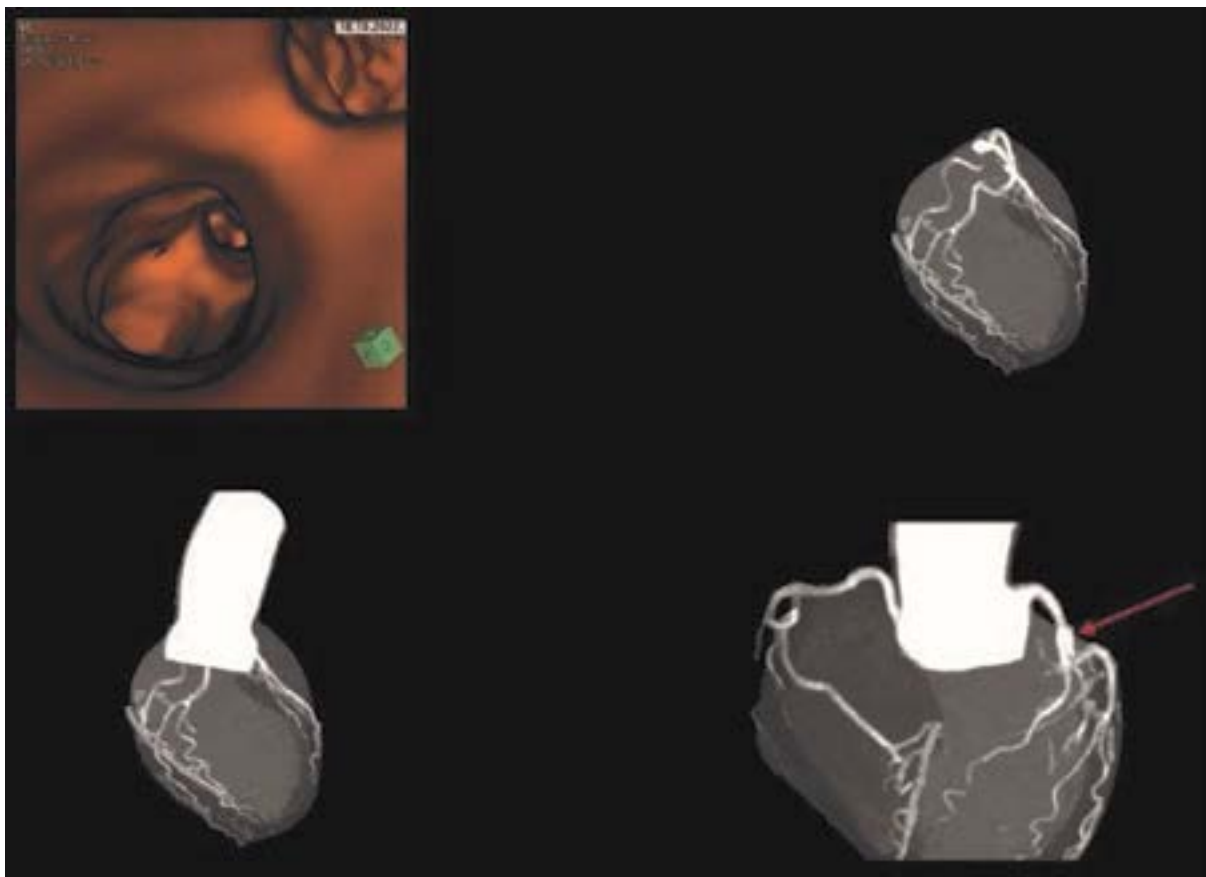
Figure 2. The software allows a semiautomatic small vessel fly-through, which provides inside front and rear views, together with a view of the path and location on the surface of the heart
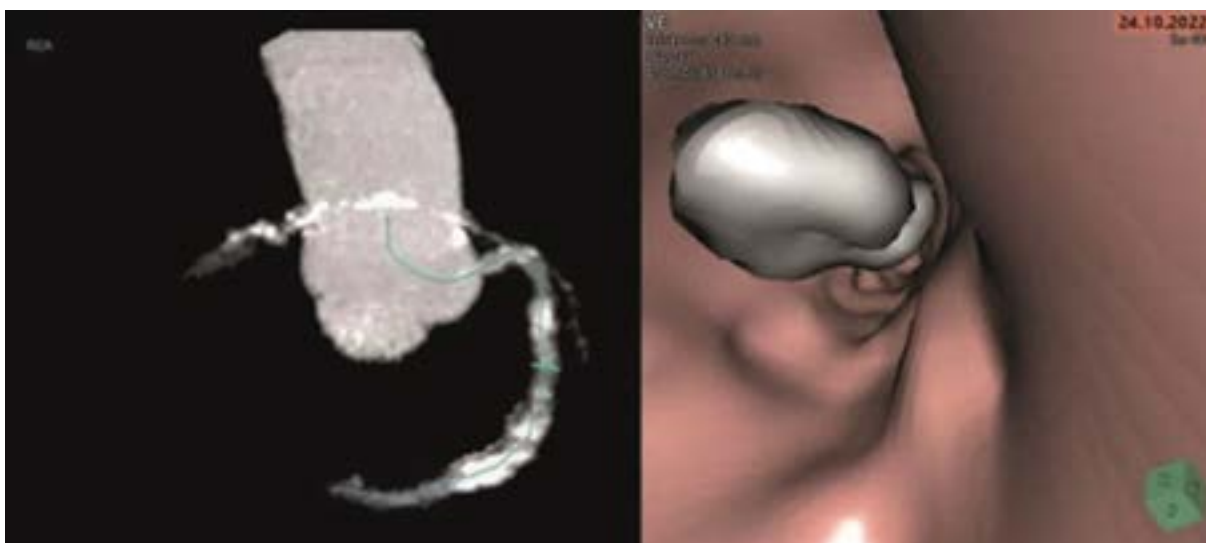

Figure 3. 3DIE visualization of non-calcified plaque. A. Curved planar reformatted image shows non-calcified plaque (arrow) at the proximal segment of LAD in a 67-year-old man. B. Corresponding 3DIE shows the plaque arising from the inferior wall of LAD with smooth appearance
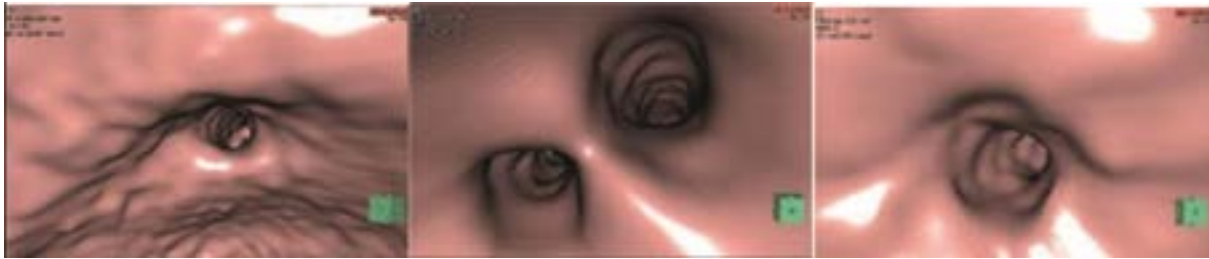
Figure 4. Depicts the normal intraluminal appearance of the left main artery (a), left coronary ostia corresponding to various branches arising from the left coronary artery (b), and the normal right coronary ostium (c) as seen on 3DIE visualization.
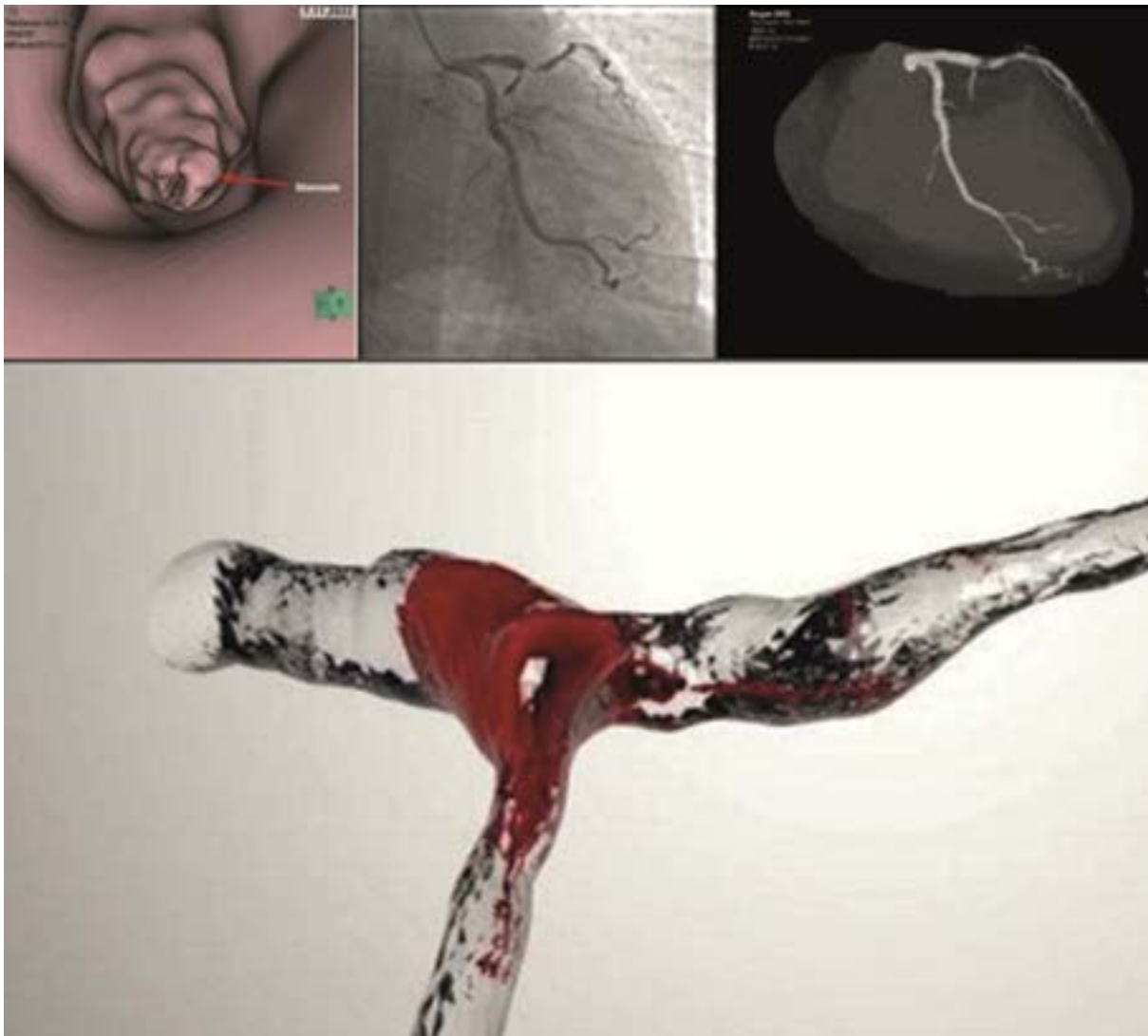

Figure 5. 3DIE visualization of non-calcified plaque (a). DSA and curved planar reformatted image show non-calcified plaque at the proximal segment (segment #7) of LAD in a 52-year-old male. (b). 3D model with flow analysis of non-calcified stenosis (c).
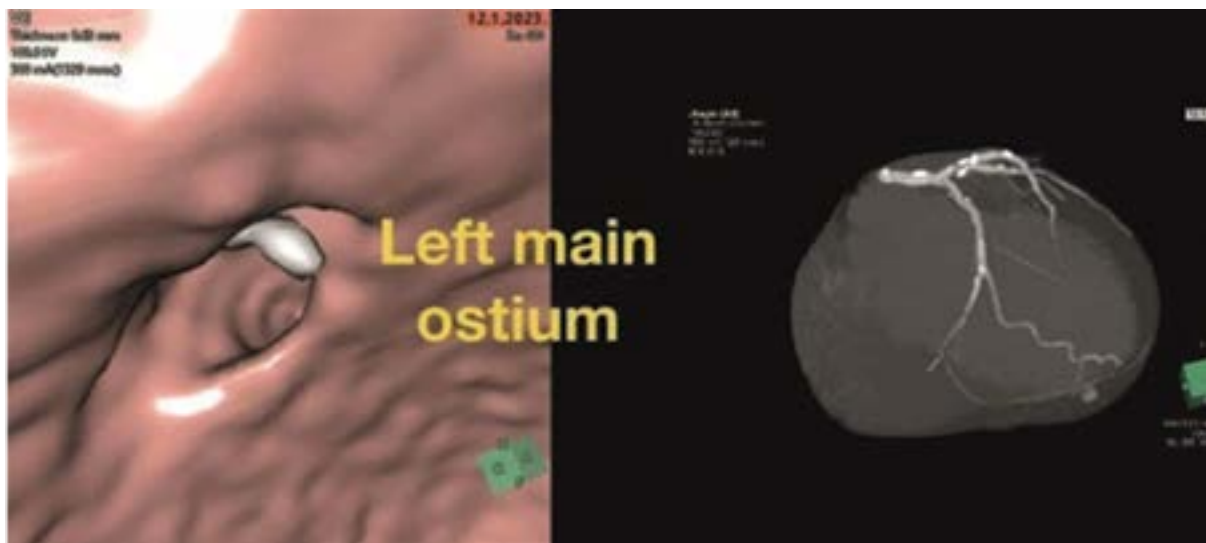
Figure 6. 3DIE visualization of eccentric calcified plaque. 3DIE shows the calcified plaque arising from the superior wall of LAD with involvement of LAD ostium. 3D reformatted image reveals calcified plaques at the left main stem and LAD coronary arteries in a 68 -year-old male
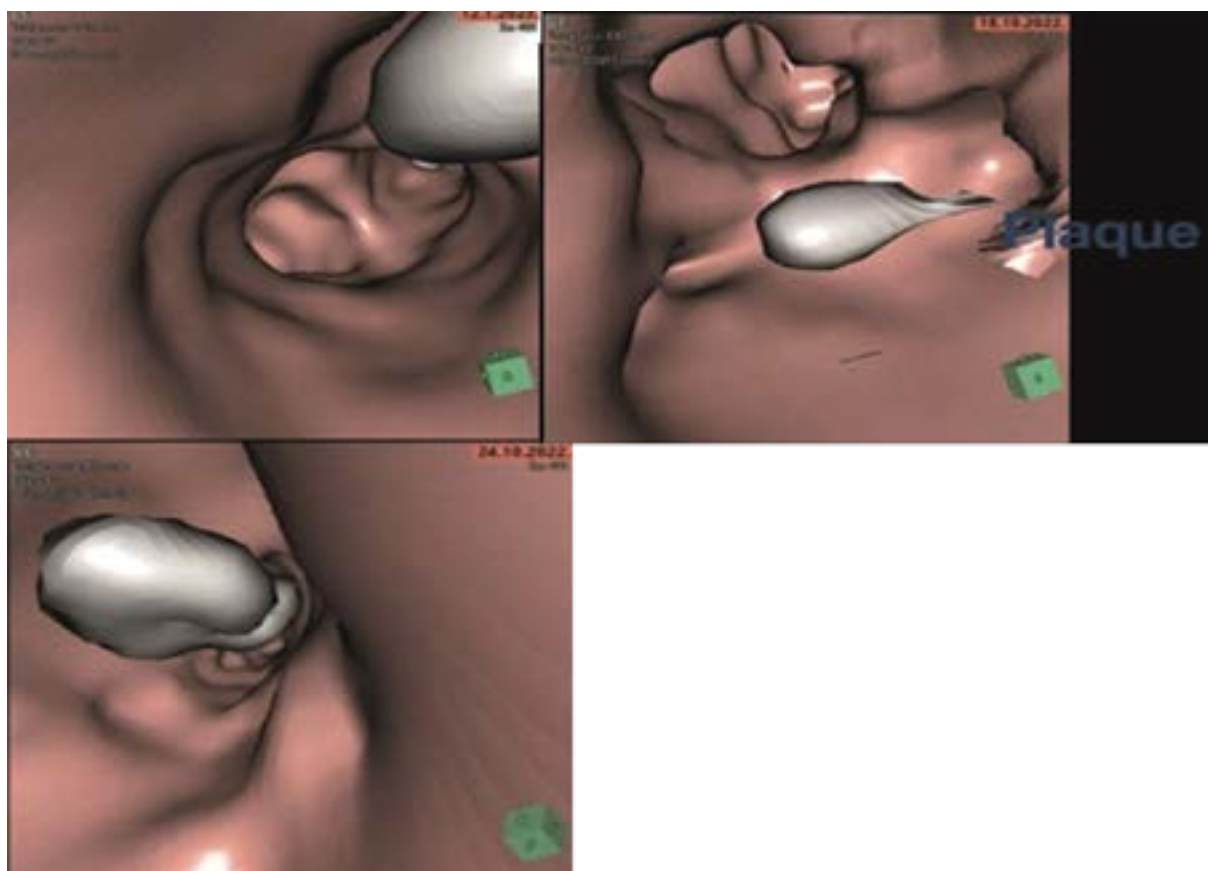

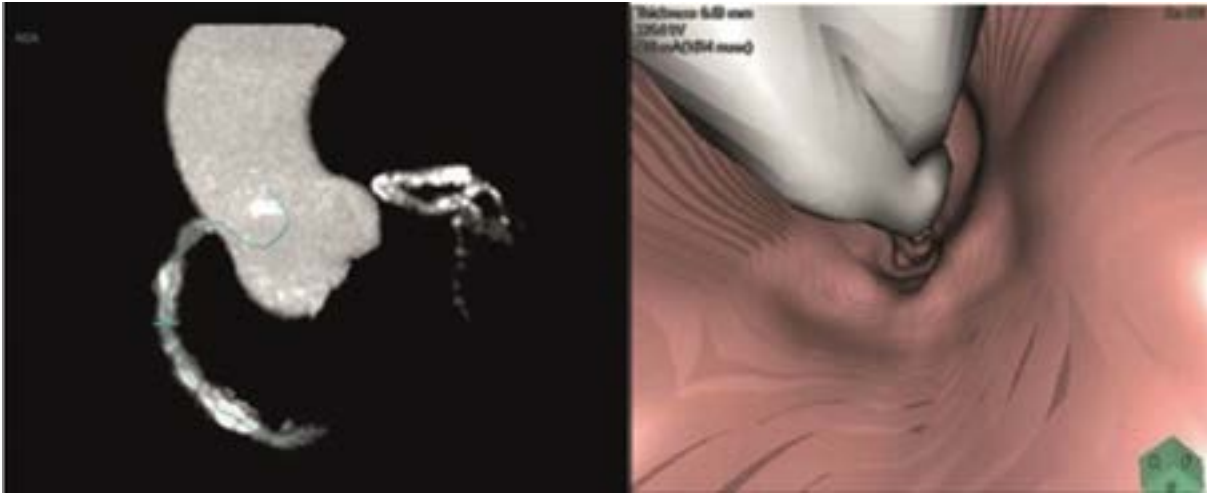Figure 7. 3DIE visualization of eccentric calcified plaques

Figure 8. 3DIE visualization of extensively calcified plaques. 3D reformatted image shows extensively calcified plaques in the RCA, LM, LAD and LCX in a 54-year-old male. (a). Corresponding 3DIE demonstrates irregular coronary lumen changes caused by the extensively calcified plaques (b)

Figure 9. 3DIE visualization of mixed plaques. 3D reformatted image shows mixed plaques with spotty calcification at the proximal segment of LAD in a 63-year-old male. 3DIE indicates irregular coronary wall changes due to different components within the plaques.
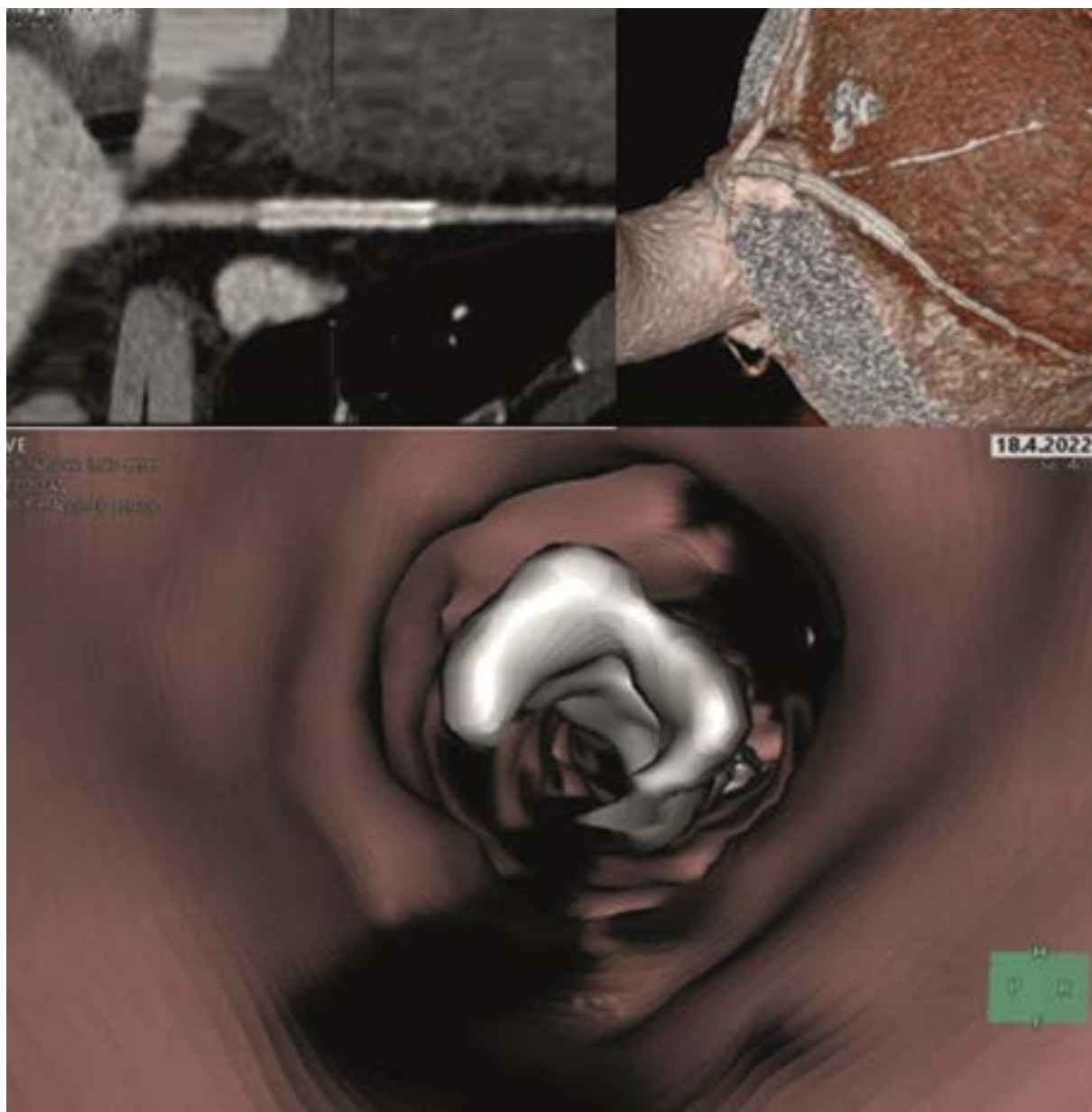
Figure 10: Visualization of functional coronary stents using 3DIE. (a) A curved planar reformatted picture reveals a 56- year-old man's patent coronary stent in the LAD. (b) Coronary stent visualization using VR. (c) Stent surface close-up 3DIE visualization reveals a smooth, circular appearance inside the RCA.

Table 1. Patient characteristics and cardiovascular risk factors

Characteristic	
Age (years) (mean (SD); range)	57 (10); 41 to 71
Male	82%
Smoking	66%
Diabetes mellitus	25%
Hyperlipidaemia	74%
Hypertension	69%
Body mass index (kg/m2) (mean (SD))	28 (3)
Family health history	45%